

# A new sol-gel route to prepare dense $\text{Al}_2\text{O}_3$ thin films



Baofu Hu<sup>\*</sup>, Erguang Jia, Baoli Du, Yuehong Yin<sup>\*</sup>

School of Physics and Electronic Information Engineering, Henan Polytech University, Jiaozuo 454000, China

## ARTICLE INFO

### Article history:

Received 19 June 2016

Received in revised form

22 July 2016

Accepted 26 July 2016

Available online 27 July 2016

### Keywords:

Sol-gel

$\text{Al}_2\text{O}_3$  films

Spin-coating

Chelating agent

## ABSTRACT

A new sol-gel route has been applied to synthesize dense  $\text{Al}_2\text{O}_3$  thin films from aluminum isopropoxide ( $\text{Al}(\text{OPri})_3$ ) as raw precursor material. The results show that, in the solution, acetylacetone (AcAc) and aluminum form a complex compound which effectively suppresses the growth of colloidal particles and makes the sol very stable.  $\text{Al}_2\text{O}_3$  thin films fabricated by spin-coating method and calcined at 500 °C for 3 h possess an amorphous structure and exhibit a highly homogeneous surface texture without evidence of holes or cracks throughout the film. Moreover, the prepared films display a low leakage current and a high transmittance. This new sol-gel route appears to be a highly promising method to synthesize dense  $\text{Al}_2\text{O}_3$  thin films from  $\text{Al}(\text{OPri})_3$ , and could provide a wide range of optical and electric applications.

© 2016 Published by Elsevier Ltd and Techna Group S.r.l.

## 1. Introduction

$\text{Al}_2\text{O}_3$  thin films have received much attention for their excellent mechanical, optical and electrical properties [1]. During the past few years  $\text{Al}_2\text{O}_3$  thin films have been widely used in optical lenses and windows, antireflection coatings [2], optical wave guides [3], microelectronic devices, opto-electronic devices, and also for the passivation of metal surfaces [4]. For most applications, much effort has been directed to obtain high-quality  $\text{Al}_2\text{O}_3$  thin films using a variety of processes such as chemical vapor deposition [5], spray pyrolysis [6], electron beam evaporation [7], magnetron sputtering [8], anodization [9], sol-gel [10,11], pulsed laser deposition [12] and atomic layer deposition [13]. Among these techniques, the sol-gel method is a particularly attractive route due to its simplicity, cost-effectiveness and to the possibility of highly control the composition of the target material. Therefore, in this paper, efforts are directed to fabricate crack-free and dense  $\text{Al}_2\text{O}_3$  thin films by exploiting a new sol-gel route. The morphology of the films has been characterized by atomic force microscopy (AFM) and field-emission scanning electron microscopy (FE-SEM). The reaction mechanisms of the sol-gel process have been studied by means of Fourier transform infrared spectroscopy (FTIR), differential scanning calorimetry (DSC) and thermogravimetry (TG) techniques. The leakage current and the transmittance of  $\text{Al}_2\text{O}_3$  thin films have also been measured in the present work.

## 2. Experimental

All chemicals used in this study are of reagent-grade purity and without further purification. Initially, 0.02 M of  $\text{Al}(\text{OPri})_3$  was dissolved in 50 mL of 2-ethoxyethanol and stirred for 30 min. Then, acetylacetone (AcAc) was added and stirred for another 30 min. At last, a small amount of (10 mL) glacial acetic acid was added to the mixture solution and then stirred for 2 h to obtain the clear and transparent pale yellow solution. The molar ratio of AcAc to  $\text{Al}(\text{OPri})_3$  was 1:1. The whole synthesis process was performed at 105 °C in a saline water-bath. The concentration of the precursor solutions was finally adjusted to 0.4 mol/L by adding appropriate quantity of glacial acetic acid. The resulting solution exhibited remarkable stability.

Two kinds of substrates, fused quartz and platinized silicon (Pt/Ti/SiO<sub>2</sub>/Si) wafers, have been used in this work. Before depositing the  $\text{Al}_2\text{O}_3$  coating, the substrates have been cleaned thoroughly by ultrasonication in acetone, ethanol and deionized water, successively, and then blow dried with N<sub>2</sub>. Spin-coating technique at 3000 rpm for 20 s was employed to deposit the sol on the substrates. Etch layer was dried at 200 °C for 10 min just after coating and then pyrolyzed at 400 °C for 10 min. The above process was repeated for several times until the desired film thickness was achieved. The spin-coating procedure was performed in a clean-room environment. Finally, the samples were calcined at 500 °C for 3 h at a heating rate of 5 °C/min in a muffle furnace to form the  $\text{Al}_2\text{O}_3$  films. The synthesis procedure for  $\text{Al}_2\text{O}_3$  films from the precursor solution is shown in Fig. 1.

The chemical processing of the sol was investigated by FTIR (Nicolot 8700). The xerogel was examined by thermal analysis (STA449C). The  $\text{Al}_2\text{O}_3$  film microstructure was characterized by FE-SEM (FEI Quanta 200 FEG). AFM (SPA-400) was used to obtain

<sup>\*</sup> Corresponding authors.

E-mail addresses: [wlbhf@hpu.edu.cn](mailto:wlbhf@hpu.edu.cn) (B. Hu), [yuehongyin@126.com](mailto:yuehongyin@126.com) (Y. Yin).

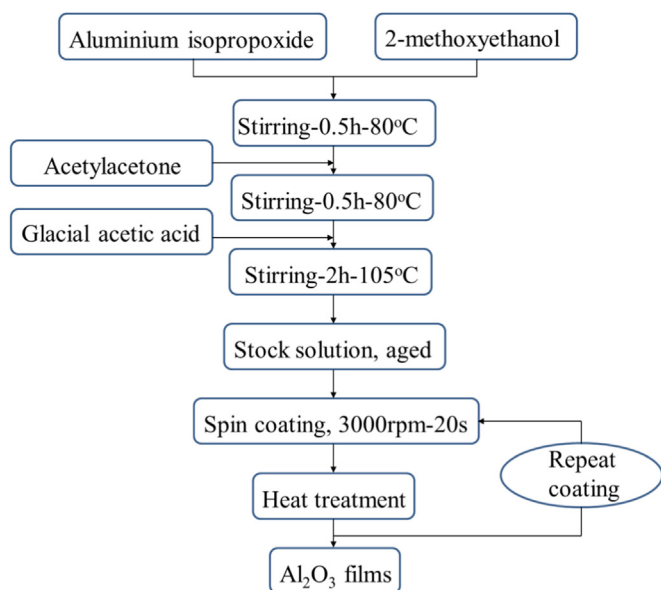


Fig. 1. Process flowchart for the synthesis of  $\text{Al}_2\text{O}_3$  films.

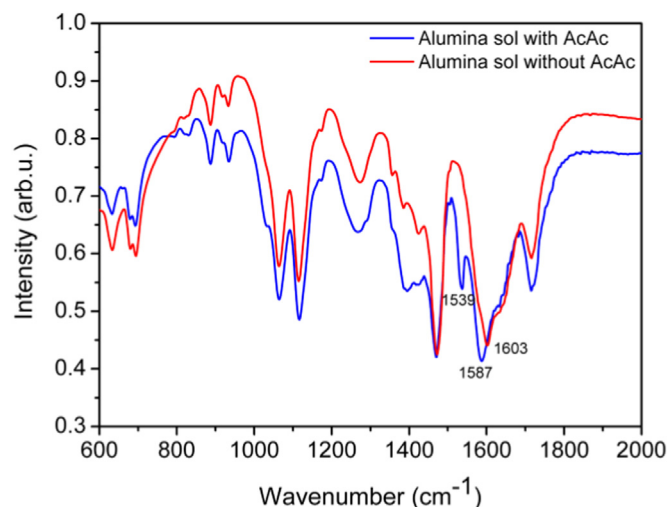


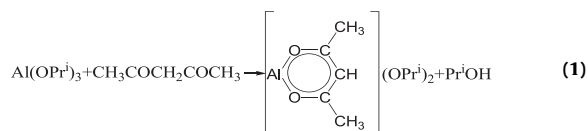
Fig. 2. FTIR spectra of  $\text{Al}_2\text{O}_3$  sol with or without AcAc.

three-dimensional images of the final sample surface. The phase structure of  $\text{Al}_2\text{O}_3$  films was identified by X-ray diffraction (BRUKER D8 Advance diffractometer). For electrical measurement, Au top electrode pads of 1 mm in diameter were sputtered through a shadow mask onto  $\text{Al}_2\text{O}_3$  thin films by DC magnetron sputtering technique. The leakage current density versus the electric field ( $J$ - $E$ ) characteristics was measured using a Keithley 2410 electrometer. A UV-VIS-NIR Spectrophotometer (Cary 5000) was finally used to record films transmission spectra in the 200 nm–1200 nm wavelength range.

### 3. Results and discussion

#### 3.1. Sol solution and xerogel analysis

To obtain stable solution, the starting material  $\text{Al}(\text{OPr}^i)_3$  is dissolved into 2-ethoxyethanol. It is well known that  $\text{Al}^{3+}$  is easily hydrolyzed in an aqueous solution. Then AcAc, as chelating agent, is added to the solution to prevent the hydrolysis and the condensation of aluminum by quickly forming a gel network thanks to the strong chelating ability of AcAc with aluminum. Based on a previous study [14], a small amount of glacial acetic acid is added to the solution to improve the quality of the sol. Acetic acid not only enhances the peptization and stabilizes the sol against gelation, by enabling strong intermolecular hydrogen bonding, but also plays an important role as a solvent. Furthermore, the resulting metal oxohydroxocarboxylates are solvated by the acetic acid [15]. The reaction between  $\text{Al}(\text{OPr}^i)_3$  and AcAc may be inferred as follows:



To further assess the validity of this reaction mechanism, the chemical process of sol is investigated by FTIR spectra. The FTIR spectra of the sol are shown in Fig. 2. As it is well known, AcAc displays both ketonic and enolic structure forms. In the FTIR spectrum of AcAc, two characteristic peaks around  $1700 \text{ cm}^{-1}$  and

$1620 \text{ cm}^{-1}$  can be assigned to the C=O stretching vibrations of ketonic and enolic forms, respectively [16]. However, as shown in Fig. 2, we do not observe these two characteristic peaks when AcAc is added to the solution. Instead, a new peak located at  $1539 \text{ cm}^{-1}$  emerges and the peak at  $1603 \text{ cm}^{-1}$  shifts to  $1587 \text{ cm}^{-1}$ . The peak at  $1587 \text{ cm}^{-1}$  can be assigned to C–O bonding with Al to form a complex, and the  $1539 \text{ cm}^{-1}$  peak to C–C bonds of the six-membered ring of the complex [16,17]. We conclude that AcAc can directly chelate with metal alkoxide molecules in an organic medium and form a chelate complex which may cause the observed red-shifts of IR absorption peaks [18,19]. The formation of a complex compound prevents hydrolysis and condensation of aluminum.

Optical photos of the sol and the corresponding spin-coated films are shown in Fig. 3. The  $\text{Al}_2\text{O}_3$  sol without AcAc results in an emulsion form composed of a suspension of small particles in a liquid. The corresponding spin-coated film is highly inhomogeneous with many particles or bigger colloidal particles. On the other hand, the sol with AcAc displays a very clear and transparent bright yellow solution, and the spin-coated films are smooth, uniform and cracks-and particles free. As mentioned above, AcAc molecules can easily chelate with  $\text{Al}^{3+}$  ions to form a complex compound. As a result, the reactive HO–Al-groups on the colloidal particles result to be sufficiently capped so that the growth of the colloidal particles is effectively prevented. This results in a very stable and transparent sol [20].

Fig. 4 gives the TG and DSC curves of the xerogel derived from the aluminum isopropoxide precursor baked at  $100^\circ\text{C}$  and grinded. The small weight losses occurring at  $73^\circ\text{C}$  and  $148^\circ\text{C}$ , correspond to the desorption of the adsorbed moisture and the solvent evaporation. A larger weight loss then occurs within the temperature range from  $290^\circ\text{C}$  to  $450^\circ\text{C}$ , this is mainly due to the decomposition of the organic groups within the xerogel. No crystallization peaks are observed below  $800^\circ\text{C}$ . At about  $870^\circ\text{C}$  a small exothermic peak occurs due to the crystallization process of alumina. The above results indicate that there is no apparent mass change above  $500^\circ\text{C}$ , suggesting that the complete decomposition of the organic groups takes place below  $500^\circ\text{C}$ .

#### 3.2. Structure and morphology of alumina films

XRD patterns of  $\text{Al}_2\text{O}_3$  thin films calcined for 3 h at a temperature from  $500^\circ\text{C}$  to  $700^\circ\text{C}$  are shown in Fig. 5. No apparent diffraction peaks can be identified in the XRD pattern even after being calcined at  $700^\circ\text{C}$ , suggesting that, in agreement with the

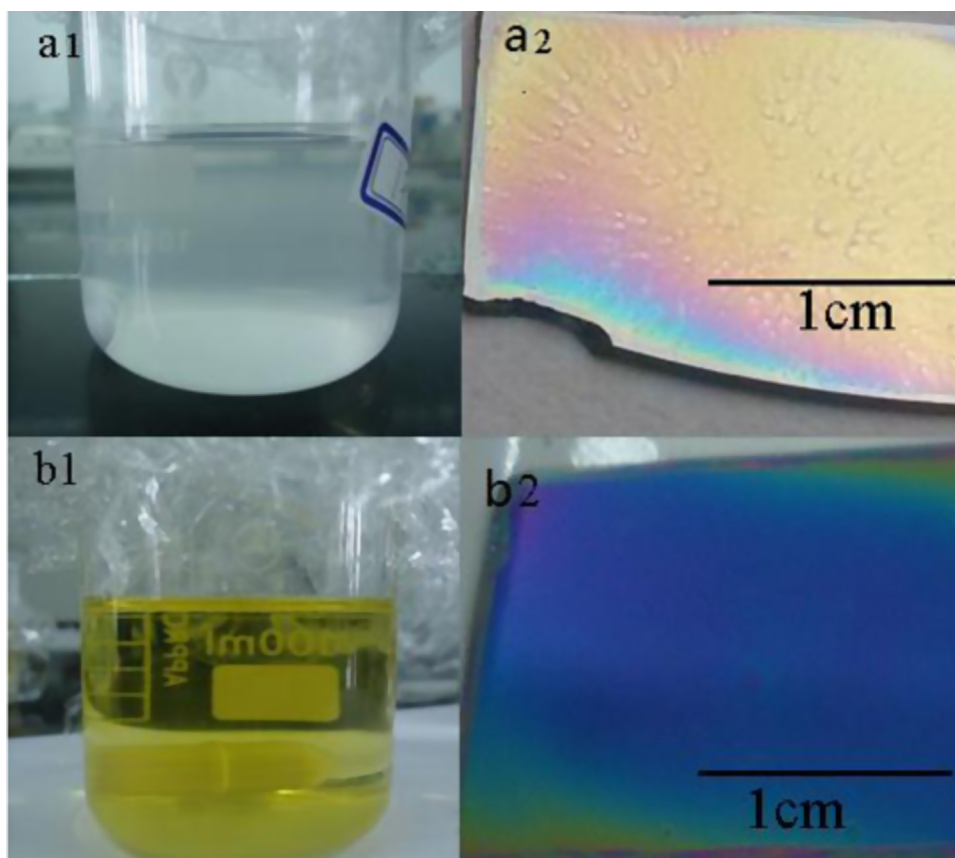


Fig. 3. Optical photos of the sol without (a) or with (b) AcAc and the corresponding spin-coated films deposited on Si substrates.

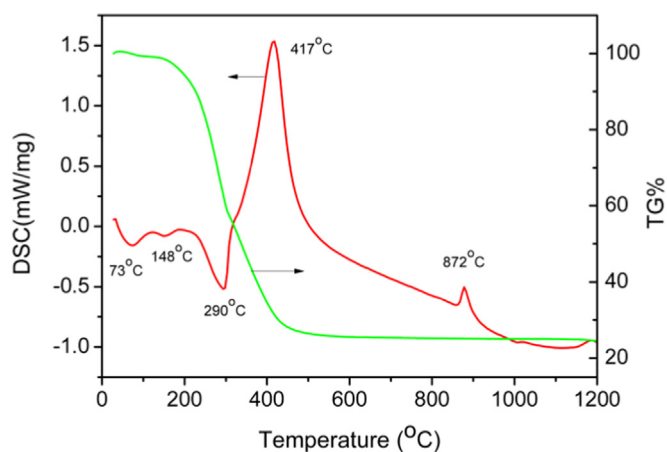


Fig. 4. TG and DSC curves of the  $\text{Al}_2\text{O}_3$  xerogel powder.

TG-DSC analyses results of Fig. 4,  $\text{Al}_2\text{O}_3$  thin films possess an amorphous structure.

Surface and cross-section morphology of the films calcined at 500 °C for 3 h were investigated by FE-SEM and AFM. As shown in Fig. 6,  $\text{Al}_2\text{O}_3$  film provides a good coverage for the Pt substrate surface. The films are extremely flat and uniform as well as crack-free. Moreover, a sharp interface is found between the dielectric layer and the substrate surface. The film thickness is evaluated to be approximately 300 nm. AFM images of an  $\text{Al}_2\text{O}_3$  film calcined at 500 °C for 3 h are shown in Fig. 7, revealing a smooth, cracks and voids free, densely packed film surface. Meanwhile, no apparent grain or grain boundaries are found, confirming that the  $\text{Al}_2\text{O}_3$  film structure is amorphous. The surface average root mean square roughness (RMS) was calculated using the equipment's software

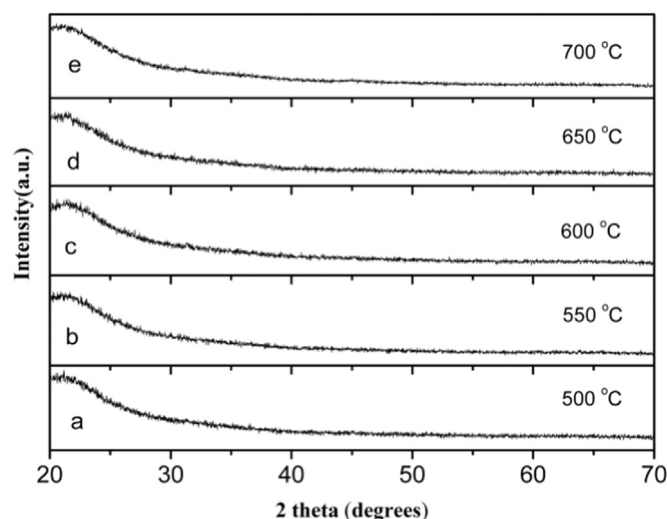


Fig. 5. XRD patterns of  $\text{Al}_2\text{O}_3$  films calcined at 500 °C to 700 °C for 3 h.

routine. The RMS value on a  $5 \times 5 \mu\text{m}$  image is approximately 0.83 nm, indicating that the films are comparable to those obtained by the atomic layer deposition and electron beam evaporation methods [21,22].

### 3.3. Electrical and optical properties of $\text{Al}_2\text{O}_3$ films

In optical-electric materials, the insulating property and the optical transmittance are two important factors: the leakage current and the transmittance of  $\text{Al}_2\text{O}_3$  films were thus accurately investigated. Fig. 8 shows the typical behavior of  $J$ - $E$  characteristics

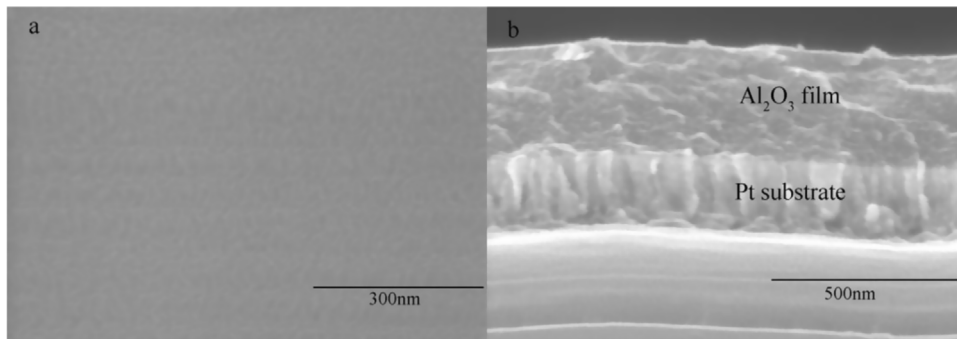


Fig. 6. FE-SEM micrograph of surface (a) and cross section (b) of an  $\text{Al}_2\text{O}_3$  film.

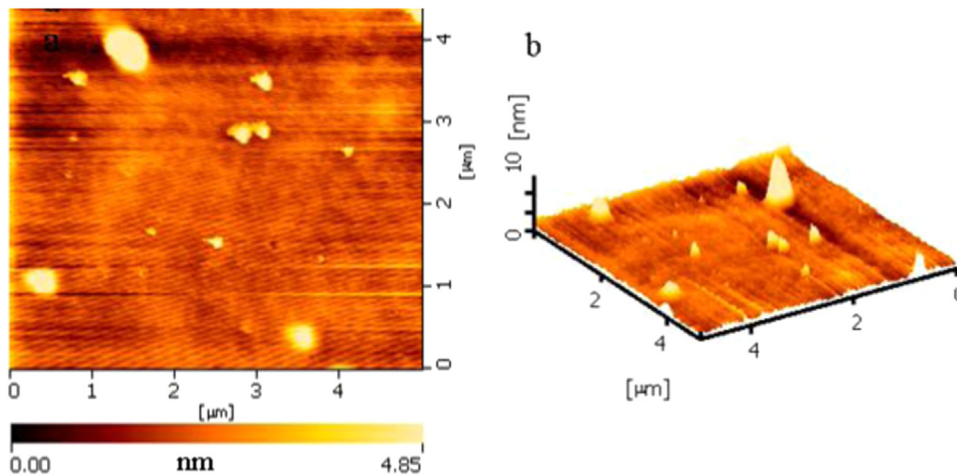


Fig. 7. AFM image of an  $\text{Al}_2\text{O}_3$  film calcined at 500 °C for 3 h.

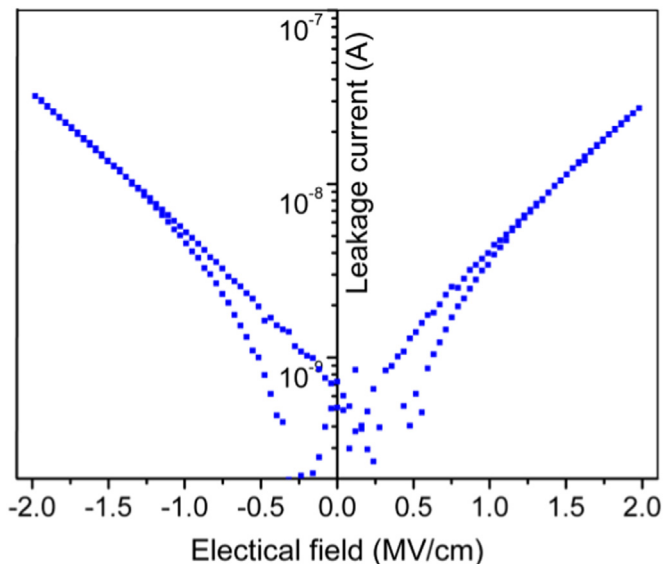


Fig. 8. Leakage current ( $J$ ) versus electrical field ( $E$ ) of  $\text{Al}_2\text{O}_3$  films on Pt substrate.

obtained in an  $\text{Al}_2\text{O}_3$  thin film calcined at 500 °C for 3 h.

The curve denotes the absolute value of the leakage current measured in an electric field (sweeping the voltage:  $-60\text{ V}$   $0\text{ V}$   $+60\text{ V}$ ). The absolute current curve shows a nearly symmetrical characteristic. The leakage current gradually increases up to  $4 \times 10^{-8}\text{ A}$  for the electrical field value of about  $2\text{ MV cm}^{-1}$ . This is

indicates that the films have a good insulating property. The cusps in the absolute current curve corresponding to a switch in polarity are not at  $0\text{ V}$ , but at about  $\pm 6\text{ V}$ . At about  $6\text{ V}$  ( $-6\text{ V}$ ), the leakage current reaches a minimum value, and then switches its polarity. We deduce that the shift of the current cusp may originate from the space charges trapped in the films [23].

To gain information on optical properties of the films, the optical transmittance of  $\text{Al}_2\text{O}_3$  films deposited on quartz was recorded in the wavelength range from 200 nm to 1200 nm (as shown in Fig. 9). The transmittance spectrum was recorded using an uncoated virgin quartz substrate as a reference. In Fig. 9, it can be observed that the films transmittance is higher than 92% in the wavelength range from 300 nm to 1200 nm. The most relevant optical parameter, the band gap  $E_g$ , was calculated using the following equation [24,25]:

$$(\alpha h\nu)^2 = A(h\nu - E_g) \quad (2)$$

where  $\alpha$  is the absorption coefficient and  $A$  is a constant.

A plot of  $(\alpha h\nu)^2$  vs.  $h\nu$  is shown in the inset of Fig. 9. The extrapolation of the linear part of the graph to  $\alpha=0$  allows determining the optical band gap of 5.06 eV. It is well-known that the band gap of crystal  $\text{Al}_2\text{O}_3$  film is in the order of 5.5 eV [26]. The decrease of the energy band gap value reported in present paper can be explained by the appearance of some defect levels located in the band gap [27] and due to the fact that the  $\text{Al}_2\text{O}_3$  film has an amorphous structure.



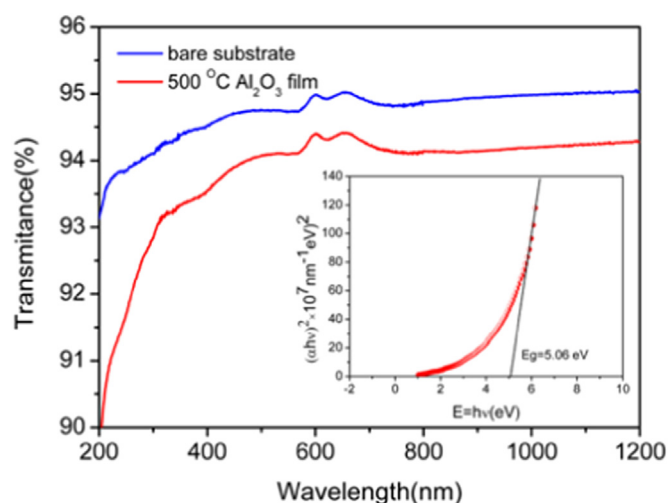


Fig. 9. Optical transmission spectra of  $\text{Al}_2\text{O}_3$  thin films on quartz, the inset shows the optical band gaps determined from the plots of  $(\alpha h\nu)^2$  vs.  $h\nu$ .

#### 4. Conclusions

In summary, we have investigated the synthesis  $\text{Al}_2\text{O}_3$  thin films starting from an alumina sol using  $\text{Al}(\text{OPr}^i)_3$  as a raw material. The resulting sol was found to be highly stable due to the formation of a complex compound in the solution. As a result, crack-free and homogeneous amorphous alumina films could be successfully deposited by a simple spin-coating method. The so fabricated  $\text{Al}_2\text{O}_3$  films show excellent optical and electrical properties. Therefore, compared with other deposition methods, the sol-gel route offers a cheap and highly promising way to deposit  $\text{Al}_2\text{O}_3$  films for many relevant applications.

#### Acknowledgments

This work was supported by National Natural Science Foundation of China (Grant no. 51202060) and Doctoral Science Foundation of Henan Polytech University (B2016-43).

#### References

- [1] G. Balakrishnan, P. Kuppusami, S.T. Sundari, R. Thirumurugesan, V. Ganesan, E. Mohandas, Structural and optical properties of  $\gamma$ -alumina thin films prepared by pulsed laser deposition, *Thin Solid Films* 518 (2010) 3898–3902.
- [2] K. Shamala, L. Murthy, M. Radhakrishna, K.N. Rao, Characterization of  $\text{Al}_2\text{O}_3$  thin films prepared by spray pyrolysis method for humidity sensor, *Sens. Actuator A Phys.* 135 (2007) 552–557.
- [3] P. Katiyar, C. Jin, R. Narayan, Electrical properties of amorphous aluminum oxide thin films, *Acta Mater.* 53 (2005) 2617–2622.
- [4] Y.-S. Chaug, N. Roy, Reactions at the aluminum oxide-ferrite interface, *Thin Solid Films* 193 (1990) 959–964.
- [5] X. Duan, N.H. Tran, N.K. Roberts, R.N. Lamb, Single-source chemical vapor deposition of clean oriented  $\text{Al}_2\text{O}_3$  thin films, *Thin Solid Films* 517 (2009) 6726–6730.
- [6] B.P. Dhonge, T. Mathews, S.T. Sundari, C. Thiraharan, M. Kamruddin, S. Dash, Spray pyrolytic deposition of transparent aluminum oxide ( $\text{Al}_2\text{O}_3$ ) films, *Appl. Surf. Sci.* 258 (2011) 1091–1096.
- [7] D.W. Thompson, P.G. Snyder, L. Castro, L. Yan, P. Kaipa, J.A. Woollam, Optical characterization of porous alumina from vacuum ultraviolet to mid infrared, *J. Appl. Phys.* 97 (2005) 113511–113519.
- [8] T. Hübert, S. Svoboda, B. Oertel, Wear resistant alumina coatings produced by a sol-gel process, *Surf. Coat. Technol.* 201 (2006) 487–491.
- [9] V. Gianneta, A. Nassiopoulou, C. Krontiras, S. Georga, Porous anodic alumina thin films on Si: interface characterization, *Phys. Status Solidi (C)* 5 (2008) 3686–3689.
- [10] T. Wang, J. Pu, C. Bo, L. Jian, Sol-gel prepared  $\text{Al}_2\text{O}_3$  coatings for the application as tritium permeation barrier, *Fusion Eng. Des.* 85 (2010) 1068–1072.
- [11] K. Vanbesien, P. De Visschere, P. Smet, D. Poelman, Electrical properties of  $\text{Al}_2\text{O}_3$  films for TFEL-devices made with sol-gel technology, *Thin Solid Films* 514 (2006) 323–328.
- [12] F. Di Fonzo, D. Tonini, A.L. Bassi, C. Casari, M. Beghi, C. Bottani, Growth regimes in pulsed laser deposition of aluminum oxide films, *Appl. Phys. A* 93 (2008) 765–769.
- [13] M. Groner, S. George, R. McLean, P. Garcia, Gas diffusion barriers on polymers using  $\text{Al}_2\text{O}_3$  atomic layer deposition, *Appl. Phys. Lett.* 88 (2006) 051903–051907.
- [14] N. Bahlawane, Novel sol-gel process depositing  $\alpha$ - $\text{Al}_2\text{O}_3$  for the improvement of graphite oxidation-resistance, *Thin Solid Films* 396 (2001) 126–130.
- [15] W. Glaubitt, W. Watzka, H. Scholz, D. Sporn, Sol-gel processing of functional and structural ceramic oxide fibers, *J. Sol-Gel Sci. Technol.* 8 (1997) 29–33.
- [16] Q. Fu, C.-B. Cao, H.-S. Zhu, Preparation of alumina films from a new sol-gel route, *Thin Solid Films* 348 (1999) 99–102.
- [17] R. Jain, A. Rai, R. Mehrotra, Synthesis and spectral studies of  $\beta$ -diketone and  $\beta$ -ketoester derivatives of aluminium zirconium isopropoxide, *Polyhedron* 5 (1986) 1017–1021.
- [18] K. Shinmou, N. Tohge, T. Minami, Fine-patterning of  $\text{ZrO}_2$  thin films by the photolysis of chemically modified gel films, *J. J. Appl. Phys.* 33 (1994) 1181–1184.
- [19] N. Tohge, K. Shinmou, T. Minami, Effects of UV-irradiation on the formation of oxide thin films from chemically modified metal-alkoxides, *J. Sol-Gel Sci. Technol.* 2 (1994) 581–585.
- [20] C. Jing, X. Zhao, Y. Zhang, Sol-gel fabrication of compact, crack-free alumina film, *Mater. Res. Bull.* 42 (2007) 600–608.
- [21] W. Cho, K. Sung, K.-S. An, S.S. Lee, T.-M. Chung, Y. Kim, Atomic layer deposition of  $\text{Al}_2\text{O}_3$  thin films using dimethylaluminum isopropoxide and water, *J. Vac. Sci. Technol. A* 21 (2003) 1366–1370.
- [22] G.W. Hyung, J. Park, J.-R. Koo, Z.-H. Li, S.J. Kwon, E.-S. Cho, Improved performance of pentacene thin-film transistors with  $\text{Al}_2\text{O}_3$  gate dielectric: annealing effect on the surface properties, *J. J. Appl. Phys.* 51 (2012) 025702–025706.
- [23] M.J. Hanna, H. Zhao, J.C. Lee, Poole Frenkel current and Schottky emission in SiN gate dielectric in AlGaIn/GaN metal insulator semiconductor heterostructure field effect transistors, *Appl. Phys. Lett.* 101 (2012) 153504–153506.
- [24] A.B. Khatibani, S. Rozati, Synthesis and characterization of amorphous aluminum oxide thin films prepared by spray pyrolysis: effects of substrate temperature, *J. Non-Cryst. Solids* 363 (2013) 121–133.
- [25] A.B. Khatibani, S. Rozati, Growth and molarity effects on properties of alumina thin films obtained by spray pyrolysis, *Mater. Sci. Semicond. Process.* 18 (2014) 80–87.
- [26] G. Adamopoulos, S. Thomas, D. Bradley, M.A. McLachlan, T.D. Anthopoulos, Low-voltage ZnO thin-film transistors based on  $\text{Y}_2\text{O}_3$  and  $\text{Al}_2\text{O}_3$  high-k dielectrics deposited by spray pyrolysis in air, *Appl. Phys. Lett.* 98 (2011) 123503–123505.
- [27] I. Costina, R. Franchy, Band gap of amorphous and well-ordered  $\text{Al}_2\text{O}_3$  on  $\text{Ni}_3\text{Al}$  (100), *Appl. Phys. Lett.* 78 (2001) 4139–4141.